PHYSICAL REVIEW D **93,** 025028 (2016)

θ dependence in $SU(3)$ Yang-Mills theory from analytic continuation

Claudio Bonati,[*] Massimo D'Elia,[†] and Aurora Scapellato[‡]

Dipartimento di Fisica dell'Università di Pisa, Largo Pontecorvo 3, I-56127 Pisa, Italy and INFN—Sezione di Pisa, Largo Pontecorvo 3, I-56127 Pisa, Italy

(Received 15 December 2015; published 27 January 2016)

We investigate the topological properties of the $SU(3)$ pure gauge theory by performing numerical simulations at imaginary values of the θ parameter. By monitoring the dependence of various cumulants of the topological charge distribution on the imaginary part of θ and exploiting analytic continuation, we determine the free energy density up to the sixth order in θ, $f(\theta,T) = f(0,T) + \frac{1}{2}\chi(T)\theta^2(1 + b_2(T)\theta^2 + b_4(T)\theta^4 + O(\theta^6))$. That permits us to achieve determinations with improved accuracy, in particular for the higher-order terms, with control over the continuum and the infinite-volume extrapolations. We obtain $b_2 = -0.0216(15)$ and $|b_4| \lesssim 4 \times 10^{-4}$.

DOI: 10.1103/PhysRevD.93.025028

I. INTRODUCTION

The nontrivial consequences related to the possible presence of a topological parameter θ are among the most interesting properties of non-Abelian gauge theories. That enters the Euclidean Yang-Mills Lagrangian as follows:

$$\mathcal{L}_\theta = \frac{1}{4} F^a_{\mu\nu}(x) F^a_{\mu\nu}(x) - i\theta \frac{g^2}{64\pi^2} \epsilon_{\mu\nu\rho\sigma} F^a_{\mu\nu}(x) F^a_{\rho\sigma}(x), \quad (1)$$

where

$$q(x) = \frac{g^2}{64\pi^2} \epsilon_{\mu\nu\rho\sigma} F^a_{\mu\nu}(x) F^a_{\rho\sigma}(x) \quad (2)$$

is the topological charge density; θ is a superselected parameter, characterizing the vacuum as well as the other physical states of the theory. The topological charge density is odd under CP symmetry, and hence a nonzero θ value would break such symmetry explicitly.

Experimental upper bounds on θ are quite stringent ($|\theta| \lesssim 10^{-10}$); nevertheless, the dependence of quantum chromodynamics (QCD) and of $SU(N)$ gauge theories on θ enters various aspects of hadron phenomenology, a paradigmatic example being the solution of the $U_A(1)$ problem [1–3]. By CP symmetry at $\theta = 0$, the free energy density f of the theory is an even function of θ which can be parametrized as follows:

$$f(\theta,T) = f(0,T) + \frac{1}{2}\chi(T)\theta^2 s(\theta,T) \quad (3)$$

where $\chi(T)$ is the topological susceptibility, while $s(\theta,T)$ is a dimensionless even function of θ, normalized as $s(0,T) = 1$, which, assuming analyticity around $\theta = 0$, can be expanded as

$$s(\theta,T) = 1 + b_2(T)\theta^2 + b_4(T)\theta^4 + \cdots. \quad (4)$$

The dependence on θ, being related to the topological properties of the theory, is inherently nonperturbative. Therefore analytic predictions are restricted to particular regimes or effective approximation schemes [4–10]. For instance, at asymptotically high temperatures the dilute instanton gas approximation is expected to hold, which predicts $f(\theta,T) - f(0,T) \simeq \chi(T)(1 - \cos\theta)$, while regarding the low-temperature phase and the θ dependence of the ground-state energy, large-N arguments [11,12] predict the various nonlinear terms in θ^2 to be suppressed by increasing powers of $1/N$, in particular $b_{2n} \propto 1/N^{2n}$ (see e.g. Ref. [13] for a general review of the subject).

Lattice QCD represents a valid nonperturbative approach, which is based on first principles only; however the complex nature of the Euclidean action in Eq. (1) hinders direct Monte Carlo simulations at nonzero θ. Some possible, partial solutions to this problem are similar to the ones adopted for QCD at finite baryon chemical potential μ_B, where the fermion determinant becomes complex. In particular, assuming analyticity around $\theta = 0$, one can either obtain the free energy density in terms of its Taylor expansion coefficients computed at $\theta = 0$ (see Refs. [14–16] for analogous strategies at $\mu_B \neq 0$), or perform numerical simulations at imaginary values of θ [17–22] (or μ_B [23–28]) and then exploit analytic continuation.

The first strategy has been traditionally adopted for the study of θ dependence. The topological susceptibility $\chi(T)$ and the coefficients b_{2n} are proportional to the coefficients of the Taylor expansion in θ and can be directly computed in terms of the cumulants of the probability distribution at

[*]claudio.bonati@df.unipi.it
[†]massimo.delia@unipi.it
[‡]Present address: Department of Physics, University of Cyprus, P.O. Box 20537, 1678 Nicosia, Cyprus and Department of Physics, Bergische Universität Wuppertal Gaussstr. 20, 42119 Wuppertal, Germany.
scapellato.aurora@ucy.ac.cy

$\theta = 0$ of the global topological charge Q. For instance the first few terms are given by

$$\chi = \frac{\langle Q^2 \rangle_{\theta=0}}{\mathcal{V}} \tag{5}$$

where $\mathcal{V}$ is the four-dimensional volume,

$$b_2 = -\frac{\langle Q^4 \rangle_{\theta=0} - 3\langle Q^2 \rangle^2_{\theta=0}}{12\langle Q^2 \rangle_{\theta=0}}, \tag{6}$$

and

$$b_4 = \frac{[\langle Q^6 \rangle - 15\langle Q^2 \rangle \langle Q^4 \rangle + 30\langle Q^2 \rangle^3]_{\theta=0}}{360\langle Q^2 \rangle_{\theta=0}}. \tag{7}$$

As we will discuss in more detail in the following, a drawback of this approach is that the coefficients of the nonquadratic terms, b_{2n}, are determined as corrections to a purely Gaussian behavior for the probability distribution of the topological charge at $\theta = 0$. By the central limit theorem, such corrections are less and less visible as the total four-dimensional volume increases, so that a significant increase in statistics is needed, in order to keep a constant statistical error, as one tries to increase $\mathcal{V}$ in order to keep finite-size effects under control.

This problem can be avoided with the approach based on analytic continuation from an imaginary θ. In this case, one typically determines a derivative of the free energy as a function of $\theta = -i\theta_I$: for instance one has

$$\frac{\langle Q \rangle_{\theta_I}}{\mathcal{V}} = \chi\theta_I(1 - 2b_2\theta_I^2) + O(\theta_I^5) \tag{8}$$

and b_2 is obtained as a deviation from linearity of the response of the system to the external source θ_I, which is determined with no loss in accuracy as the system size is increased. A drawback in this case is represented by a finite renormalization appearing when the external source θ_I is added to the discretized theory; nevertheless, the method of analytic continuation turns out to be the most suitable to a high-precision study of the coefficients b_{2n}, which must keep both finite-size and discretization errors under control.

In this study we investigate the θ dependence of $SU(3)$ pure gauge theory using the analytic continuation approach. We will explore variants of the original strategy presented in Ref. [21], in particular we will perform a simultaneous fit to various derivatives of the free energy density as a function of θ_I, in analogy with a similar approach explored in lattice QCD at imaginary chemical potential [28]. That will permit us to maximize the information obtained from our numerical simulations and, at the same time, to determine the finite renormalization constant as a parameter of the global fit. That will result in an increased precision, which will give us the opportunity to determine a continuum extrapolated value of b_2 with an uncertainty at the level of a few percent.

II. NUMERICAL METHOD

The free energy density of Yang-Mills theory in the presence of a θ term is given by

$$e^{-\mathcal{V}f(\theta,T)} = \int [dA] e^{-(S^E_{\rm YM}[A] - i\theta Q[A])}, \tag{9}$$

where $S^E_{\rm YM}$ is the standard euclidean action of Yang-Mills theory, $Q = \int q(x)\mathrm{d}x$ is the topological charge and periodic boundary conditions are assumed. As discussed in the Introduction it is not possible to use directly this form in a Monte Carlo simulation, since the action is not real for $\theta \neq 0$. To overcome this problem we will study the theory for imaginary values of θ, where standard importance sampling methods can be applied, using the analytic continuation of Eqs. (3) and (4) to extract the values of the coefficients.

In practice, one defines $\theta \equiv -i\theta_I$, where θ_I is a real parameter, and studies the θ_I dependence of

$$\begin{aligned}\tilde{f}(\theta_I, T) &\equiv f(-i\theta_I, T) - f(0, T) \\ &= -\frac{1}{2}\chi\theta_I^2(1 - b_2\theta_I^2 + b_4\theta_I^4 + \cdots).\end{aligned} \tag{10}$$

From Eq. (9) it follows that the derivatives of $\tilde{f}$ can be written as

$$\frac{\partial^k \tilde{f}(\theta_I)}{\partial\theta_I^k} = -\frac{1}{\mathcal{V}}\langle Q^k \rangle_{c,\theta_I}, \tag{11}$$

where $\langle Q^k \rangle_{c,\theta_I}$ are the cumulants of the topological charge distribution at fixed θ_I. Since for $\theta_I \neq 0$ the CP symmetry is explicitly broken, also the odd cumulants are generically nonvanishing. Using Eq. (11) together with the expansion in Eq. (10) we obtain an infinite chain of equations relating the cumulants of the topological charge to the coefficients χ and b_{2n}. The first few of these equations are the following:

$$\begin{aligned}\frac{\langle Q \rangle_{c,\theta_I}}{\mathcal{V}} &= \chi\theta_I(1 - 2b_2\theta_I^2 + 3b_4\theta_I^4 + \cdots), \\ \frac{\langle Q^2 \rangle_{c,\theta_I}}{\mathcal{V}} &= \chi(1 - 6b_2\theta_I^2 + 15b_4\theta_I^4 + \cdots), \\ \frac{\langle Q^3 \rangle_{c,\theta_I}}{\mathcal{V}} &= \chi(-12b_2\theta_I + 60b_4\theta_I^3 + \cdots), \\ \frac{\langle Q^4 \rangle_{c,\theta_I}}{\mathcal{V}} &= \chi(-12b_2 + 180b_4\theta_I^2 + \cdots).\end{aligned} \tag{12}$$

The general idea of the analytic continuation method is to perform Monte Carlo simulations at several values of θ_I, to

compute some of the cumulants $\langle Q^k \rangle_{c,\theta_I}$ for each θ_I and to extract the coefficients χ, b_{2n} making use Eq. (12).

It is clear that in this procedure one can adopt different strategies. Each of the relations in Eq. (12) is itself sufficient to extract all the parameters, at least from a given order on: for example χ can be estimated by looking at the leading linear dependence of $\langle Q \rangle_{c,\theta_I}$ on θ_I or by looking at the small θ_I value of $\langle Q^2 \rangle_{c,\theta_I}$. While all these methods are equally valid from the theoretical point of view, they are not equivalent in computational efficiency, since at fixed statistics lower cumulants are determined with better accuracy (see Sec. III A for a detailed discussion on this point). On the other hand the computation of higher cumulants does not require new simulations or even new measurements, so that if we use *also* higher momenta we increase the information available at no additional cost. What appears to be the optimal strategy is to extract χ and b_{2n} from a combined fit of all the relations in Eq. (12). Since higher momenta get more and more noisy, it is natural to expect that, at some point, adding to the global fit still higher cumulants will not result in an increased precision; however it is not *a priori* clear when this will happen and in the following analysis we will use up to the fourth cumulant. Obviously, in order to correctly assess the statistical uncertainties of the extracted parameters, correlations among the cumulants have to be taken into account.

A. Lattice implementation and topological charge definition

Various methods exist to determine the topological content of lattice configurations, either based on fermionic or gluonic definitions, which have proven to provide consistent results as the continuum limit is approached (see Ref. [13] for a review). Gluonic definitions are typically affected by renormalizations related to fluctuations at the ultraviolet cutoff scale, which can be cured by a proper smoothing of gauge configurations. Cooling [29–33] is a standard procedure adopted to do that; recently the gradient flow [34,35] has been introduced, which has been shown to provide results equivalent to cooling, at least regarding topology [36–39].

However, for the purpose of inserting a θ term in the action, the use of a fermionic or of a smoothed gluonic definition of Q is impractical. The lattice partition function in the presence of an imaginary θ term reads

$$Z_L(T,\theta_L) = \int [dU] e^{-S_L[U]+\theta_L Q_L[U]}, \tag{13}$$

where U stands for the gauge link variables, $U_\mu(n)$, S_L is the lattice pure gauge action and $Q_L = \sum_x q_L(x)$ is the discretized topological charge. Standard efficient algorithms like the heat-bath algorithm, which are available for pure gauge theories, are applicable in this case only if a particularly simple discretization of the topological charge density $q_L(x)$ is chosen, while other choices would lead to a significant computational overhead. In our case, we choose the standard Wilson plaquette action for S_L and the simplest discretization of $q(x)$ with definite parity [40,41]:

$$q_L(x) = \frac{-1}{2^9\pi^2} \sum_{\mu\nu\rho\sigma=\pm 1}^{\pm 4} \tilde{\epsilon}_{\mu\nu\rho\sigma} Tr(\Pi_{\mu\nu}(x)\Pi_{\rho\sigma}(x)), \tag{14}$$

where $\Pi_{\mu\nu}$ is the plaquette operator, $\tilde{\epsilon}_{\mu\nu\rho\sigma} = \epsilon_{\mu\nu\rho\sigma}$ for positive directions, while $\tilde{\epsilon}_{\mu\nu\rho\sigma} = -\tilde{\epsilon}_{(-\mu)\nu\rho\sigma}$ and antisymmetry fix its value in the generic case. With this choice, gauge links still appear linearly in the Boltzmann weight, so that standard heat-bath and over-relaxation algorithms can be implemented, with a computational cost that is about a factor 2.5 higher than at $\theta_L = 0$.

A drawback of this choice is that $q_L(x)$ takes a finite multiplicative renormalization with respect to the continuum density $q(x)$ [42–45]

$$q_L(x) \overset{a\to 0}{\sim} a^4 Z(a) q(x), \tag{15}$$

where a is the lattice spacing and $\lim_{a\to 0} Z(a) = 1$. Hence, the lattice parameter θ_L is related to the imaginary part of θ by $\theta_I = Z\theta_L$: in order to know θ_I, one has to determine the value Z.

As for the operator used to determine the cumulants of the topological charge distribution, in order to avoid the appearance of further renormalization constants, we adopt a smoothed definition which is denoted simply as Q in the following. In particular, we adopt the topological charge density in Eq. (14), measured after 15 cooling steps. Actually, in this case two possible prescriptions can be taken. One can simply define $Q = Q_L^{\text{smooth}}$: in this case, at finite lattice spacing, Q does not take exactly integer values, although its distribution is characterized by sharp peaks located at approximately integer values. As an alternative, one can define Q as follows [46]:

$$Q = \text{round}(\alpha Q_L^{\text{smooth}}), \tag{16}$$

where round(x) denotes the integer closest to x and the rescaling factor α is determined in such a way to minimize

$$\langle (\alpha Q_L^{\text{smooth}} - \text{round}[\alpha Q_L^{\text{smooth}}])^2 \rangle, \tag{17}$$

so that the sharp peaks in the distribution of $\alpha Q_L^{\text{smooth}}$ will be located exactly onto integer values. The two definitions are expected to coincide as the continuum limit is approached. In the following we will refer to the latter as the *rounded* topological charge and to the former as the *nonrounded* one. The two definitions have been used alternately in various previous studies in the literature. In this study we consider both of them and show that, while results at finite lattice spacing differ, continuum extrapolated results coincide, as expected.

In order to make use of Eq. (12) to obtain the free energy parameters from the θ dependence of the cumulants of Q, one needs to know the values of θ_I used for each numerical simulation. That in turn requires a determination of the renormalization constant Z. Various methods exist to do that, for instance by using the relation [21]

$$Z \equiv \frac{\langle Q Q_L \rangle_{\theta=0}}{\langle Q^2 \rangle_{\theta=0}} \tag{18}$$

or other similar approaches, like heating techniques [45]. However, a drawback of this approach is that the statistical uncertainty on Z propagates to θ_I, so that a nontrivial fit with errors on both dependent and independent variables is required. For that reason in this study we investigate and adopt a different approach.

We rewrite a lattice version of Eq. (12) in which the lattice parameter θ_L appears explicitly:

$$\begin{aligned}
\frac{\langle Q \rangle}{\mathcal{V}} &= \chi Z \theta_L (1 - 2 b_2 Z^2 \theta_L^2 + 3 b_4 Z^4 \theta_L^4 + \cdots), \\
\frac{\langle Q^2 \rangle_c}{\mathcal{V}} &= \chi (1 - 6 b_2 Z^2 \theta_L^2 + 15 b_4 Z^4 \theta_L^4 + \cdots), \\
\frac{\langle Q^3 \rangle_c}{\mathcal{V}} &= \chi (-12 b_2 Z \theta_L + 60 b_4 Z^3 \theta_L^3 + \cdots), \\
\frac{\langle Q^4 \rangle_c}{\mathcal{V}} &= \chi (-12 b_2 + 180 b_4 Z^2 \theta_L^2 + \cdots).
\end{aligned} \tag{19}$$

Our proposal is to extract the renormalization constant from the fitting procedure itself, treating θ_L as the independent variable and Z as a fit parameter. Notice however that, in order to do that, at least two cumulants must be fitted simultaneously, otherwise Z remains entangled as an arbitrary multiplicative renormalization of the other fit parameters. On the other hand, fitting the dependence of more cumulants at the same time coincides with our proposed strategy to extract the best possible information from our Monte Carlo simulations. As we will show in the next section, the payoff of this strategy is not negligible.

III. NUMERICAL RESULTS

We have performed simulations at four different lattice spacings on hypercubical lattices; the values of the bare parameters adopted are reported in Tables I and II; for the statistics adopted and the final results see Tables III and IV respectively. The Monte Carlo updates were performed using a mixture of standard heat-bath [49,50] and over-relaxation [51] algorithms, implemented *à la* Cabibbo-Marinari [52], in the ratio of 1 to 5. The topological charge was measured every ten updates and from 5 to 25 cooling steps were used: data that will be presented in the following refer to the case of 15 cooling steps and we checked that results are stable, well within errors, if a different choice is made.

Unless otherwise explicitly stated, we present data which refer to the case of a common fit to the first four cumulants of the topological charge; see Eq. (19). An example of such a fit is reported in Fig. 1. Since cumulants of different order are computed on the same samples of gauge configurations, in order to take into account the possible correlations among them we have used a bootstrap procedure, and checked that a correlated fit exploiting the full covariance matrix leads to consistent results.

In the following we are going to illustrate our estimation of the various possible systematic uncertainties that may affect our results. First, we will analyze those related to analytic continuation itself, by considering the stability of our fits as either the fit range or the number of fitted terms in Eq. (19) (i.e. the truncation of the Taylor series) is changed; then we will turn to the analysis of the infinite-volume and continuum limit extrapolations. That will permit us to provide final estimates of the free energy coefficients entering Eqs. (3) and (4), with a reliable determination

TABLE I. Physical scale determination at the bare couplings used in this work, from Ref. [47]. r_0 is the Sommer parameter [48] and in the last column the lattice spacing is obtained by using $r_0 \simeq 0.5$ fm.

β	r_0/a	a [fm]
5.95	4.898(12)	0.1021(25)
6.07	6.033(17)	0.08288(23)
6.20	7.380(26)	0.06775(24)
6.40	9.74(5)	0.05133(26)

TABLE II. Bare couplings, lattice sizes and fit ranges adopted.

β	$N_t \times N_s^3$	θ_L
5.95	16^4	0,2,4,6,8
6.07	22^4	0,2,4,6,8,10
6.20	16^4, 18^4, 20^4, 22^4	0,2,4,6,8,10,12
6.40	30^4	0,2,4,6,8,10,12,14
6.173	10×40^3	0,2,4,6,8,10,12

TABLE III. Statistics used for the various lattices: the first number of the third column is the statistics for the $\theta = 0$ run, while the second is the typical statistics of the $\theta \neq 0$ runs. The estimated autocorrelation time of the topological charge is reported in the last column.

β	$N_t \times N_s^3$	# measures	$\tau(Q)$
5.96	16^4	240 K, 130 K	3.47(8)
6.07	22^4	110 K, 70 K	4.8(2)
6.20	16^4	170 K, 60 K	18(1)
6.20	18^4	100 K, 70 K	17(1)
6.20	20^4	100 K, 90 K	17(1)
6.20	22^4	110 K, 80 K	16(1)
6.40	30^4	200 K, 120 K	214(30)
6.173	10×40^3	50 K, 20 K	27(3)

TABLE IV. Results of the combined fit to Z, χ and b_2 using up to the fourth cumulant of the topological charge. A vanishing b_4 was assumed in the fit.

	rounded Q_L		
β	Z	$a^4\chi$	b_2
5.95	0.12398(31)	$1.0744(29) \times 10^{-4}$	−0.02457(84)
6.07	0.15062(62)	$4.601(22) \times 10^{-5}$	−0.02285(90)
6.20	0.1778(13)	$1.956(17) \times 10^{-5}$	−0.02258(86)
6.40	0.2083(29)	$5.94(10) \times 10^{-6}$	−0.02347(98)
	nonrounded Q_L		
β	Z	$a^4\chi$	b_2
5.95	0.13838(36)	$8.711(23) \times 10^{-5}$	−0.01761(68)
6.07	0.16300(73)	$3.940(19) \times 10^{-5}$	−0.01898(73)
6.20	0.1900(14)	$1.728(15) \times 10^{-5}$	−0.01887(71)
6.40	0.2185(28)	$5.449(88) \times 10^{-6}$	−0.02069(89)

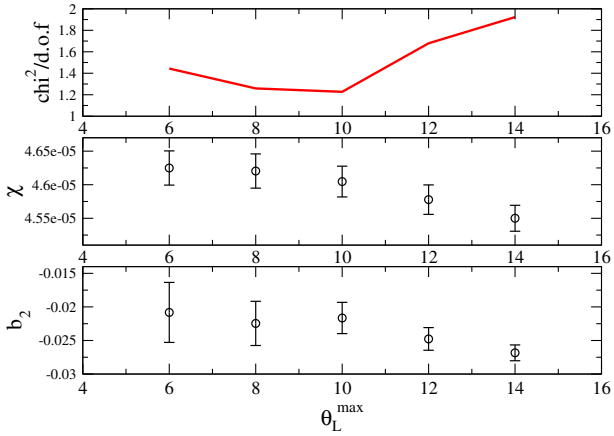

FIG. 2. An example of the variation of the fit quality and parameters with the fit range. Data refer to the 22^4 lattice at coupling $\beta = 6.07$.

of both statistical and systematic uncertainties. In the last part of our analysis we will try to understand which aspects of our strategy lead to a more significant improvement with respect to other methods used in past literature.

In Fig. 2 we report an example of how the fitted coefficients and the quality of the fit change as a function of the range of imaginary values of θ included in the fit, in particular of the maximum value $\theta_L^{\max}$. The final range from which we extract our determination is chosen so as to have a reasonable value of the χ^2/d.o.f. test and stability, within errors, of the fitted parameters as the range is reduced further: this is important to ensure the reliability of analytic continuation, since the expressions in Eq. (19) are expected to hold, in principle, in a limited range around $\theta_L = 0$. A full account of the ranges used in the various cases is reported in Table II.

We notice that $\theta_L^{\max}$ grows as one approaches the continuum limit. That can be interpreted by observing that, since growing values of θ_L induce growing values of the net nonzero topological charge density, one may expect saturation effects to be present for large enough values of θ_L. Such effects are expected to appear earlier on lattices with less resolution, i.e. with larger values of the lattice spacing.

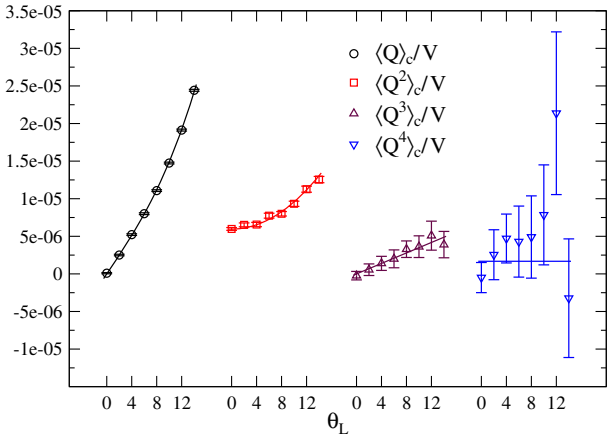

FIG. 1. An example of the global fit procedure: data refer to the 30^4 lattice at coupling $\beta = 6.40$, while continuous lines are the result of a combined fit of the first four cumulants.

A source of systematic error that is generically present in the analytic continuation approach is the one related to the choice of the fitting function, in particular to the truncation of the series to be fitted. In the present work, the estimated value of b_4 turns out to be compatible with zero for all the data sets, so it appears reasonable to fix the value of b_4 to zero and fit just Z, χ and b_2. To check that this does not introduce any significant systematic error we verified that fits with fixed $b_4 = 0$ describe the data well and give results compatible with the ones obtained by fitting also b_4.

In order to investigate finite-size effects, we have explored different lattice sizes N_s for one case, in particular $\beta = 6.2$ corresponding to a lattice spacing $a \sim 0.068$ fm. In Fig. 3 we report the corresponding results obtained both from analytic continuation and from a direct measurement of the cumulants at $\theta = 0$. We notice that errors on b_2 and b_4 obtained from analytic continuation scale much better as the volume is increased (the underlying reason is discussed in Sec. III A), so that in this case one can investigate finite-size effects with much more reliability than with a traditional approach based on $\theta = 0$ simulations only. One could try to estimate the infinite-volume limit by explicitly fitting the volume dependence of the results, which is expected to decay exponentially with N_s; however it is clearly visible from the figure that finite-size effects are negligible within errors for lattices with $N_s \geq 18$, i.e. for $N_s a > 1.2$ fm. Lattices explored at the other values of the lattice spacing have been chosen accordingly, i.e. they correspond to linear sizes which are well above this threshold (1.5 fm at least).

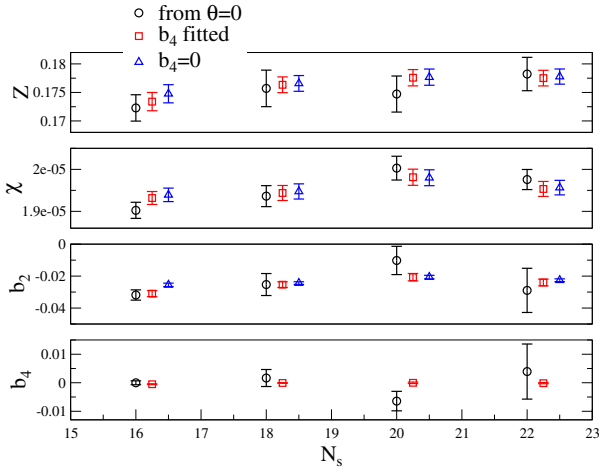

FIG. 3. Dependence of Z, χ, b_2 and b_4 on the lattice size for $\beta = 6.2$. For each lattice size and each observable three estimates are reported: the one coming just from the $\theta = 0$ simulations (i.e. the traditional Taylor expansion determination), the one obtained by fitting the b_4 value and the one obtained by fixing $b_4 = 0$.

Let us now go to a discussion of the continuum limit. In order to have better control of the systematics of the continuum extrapolation, we used two different definitions of the topological charge: the rounded and the nonrounded one (see Sec. II A). Since the two definitions are expected to coincide in the continuum limit and they were measured on the same set of gauge configurations, the differences obtained for the continuum extrapolated values in the two cases can be used as an estimate of the residual systematic uncertainties on the final results. In Fig. 4 we report results obtained for the topological susceptibility as a function of $(a/r_0)^2$, where r_0 is the Sommer scale parameter [48]. In both cases (rounded and nonrounded) finite cutoff effects can be reasonably fitted by a quadratic function of a if the three finest lattices are considered. Our final estimate is

$$r_0\chi^{1/4} = 0.4708(42)(58) \tag{20}$$

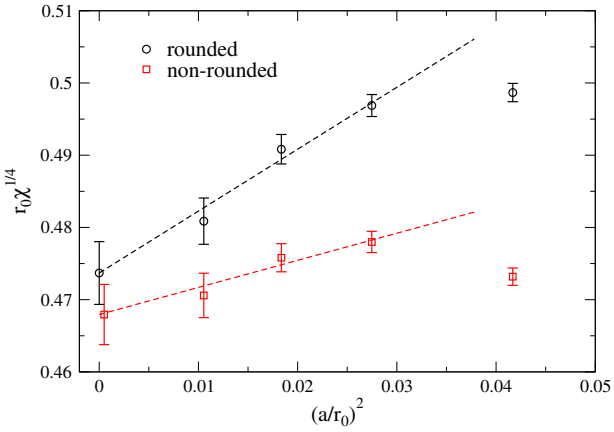

FIG. 4. Continuum limit for χ, with and without adopting a rounding to the closest integer for the topological charge measured after cooling.

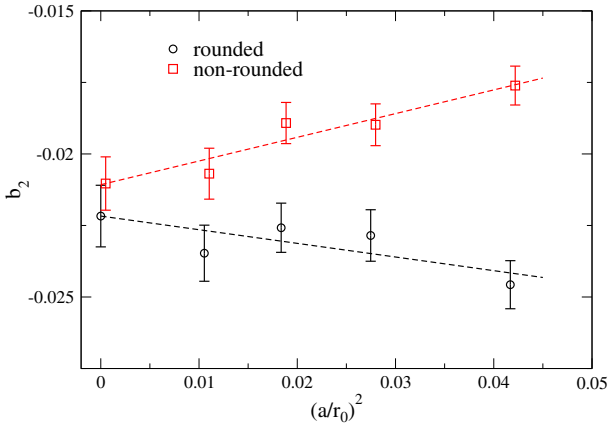

FIG. 5. Continuum limit for b_2, with and without adopting a rounding to the closest integer for the topological charge measured after cooling.

where the first error is the statistical one and the second is the systematic one; this value is compatible with previous determinations [46,53–58] and has a similar error. The conversion to physical units can be performed e.g. using $r_0 F_K = 0.293(7)$ (from Ref. [59]) and the experimental value $F_k \sim 110$ MeV, thus obtaining $\chi^{1/4} = 176.8(2.7)(4.2)$. The first error originates from the uncertainty in $r_0\chi^{1/4}$ (the systematic and statistical components were summed in quadrature), while the second error is related to the scale setting and it is the dominant one.

A similar analysis for b_2 is reported in Fig. 5. In this case our final result is

$$b_2 = -0.0216(10)(11), \tag{21}$$

where again the numbers in parentheses are, from left to right, the statistical and the systematic error. This number is compatible with previous results in the literature [21,46,58,60,61], as can be appreciated from Fig. 6 where we report a summary of all existing determinations; however a sizable error reduction has been achieved in the present study.

Finally, as we have already emphasized, we do not find any evidence of a nonvanishing b_4 coefficient, so the best we can do is to set an upper bound to its absolute value. In Fig. 7 we show the results obtained by using a combined fit for the first four cumulants, with Z, χ, b_2 and b_4 as fit parameters. All data are compatible with zero and a reasonable upper bound appears to be

$$|b_4| \lesssim 4 \times 10^{-4}. \tag{22}$$

A. Comparison with the efficiency of other approaches

As we have already emphasized, Fig. 3 shows that, at least for the higher-order cumulants, the gain in statistical accuracy obtained by analytic continuation with respect to a

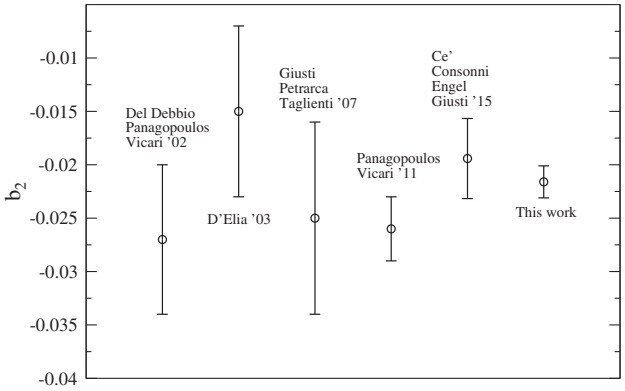

FIG. 6. Comparison of various determinations of b_2 present in the literature. From left to right: Refs. [21,46,58,60,61] and this work. The error reported for the present determination is a combination (in quadrature) of the statistical and systematic uncertainties. Notice that in Refs. [61] and [58] results were given in terms of $R = -12b_2$ and have been converted to match with the definition of the expansion coefficients used in this study.

direct determination at $\theta = 0$ becomes overwhelming as the lattice volume grows. We are now going to understand why.

The cumulants of the topological charge distribution, $\langle Q^k \rangle_c$, are proportional to the coefficients of the Taylor expansion of the free energy as a function of θ. Since the free energy is an extensive quantity, the cumulants are extensive as well, and therefore $\langle Q^k \rangle_c$ scales proportionally to the four-dimensional volume $\mathcal{V}$, and the ratios of cumulants, i.e. the coefficients b_2, b_4, … entering the free energy density, are volume independent. On the other hand, in the large-volume limit the probability distribution of the topological charge is dominated by Gaussian fluctuations with variance $\chi\mathcal{V}$, and hence the typical fluctuation has size $\delta Q \sim \sqrt{\chi\mathcal{V}}$. Since at $\theta = 0$ the distribution of Q is centered around zero, one has that the terms that sum up to $\langle Q^k \rangle_c$ (i.e. $\langle Q^k \rangle, \langle Q^2 \rangle \langle Q^{k-2} \rangle, \ldots \langle Q^2 \rangle^{k/2}$) grow like $(\chi\mathcal{V})^{k/2}$. Therefore the cumulant itself, which is of order $\chi\mathcal{V}$, comes

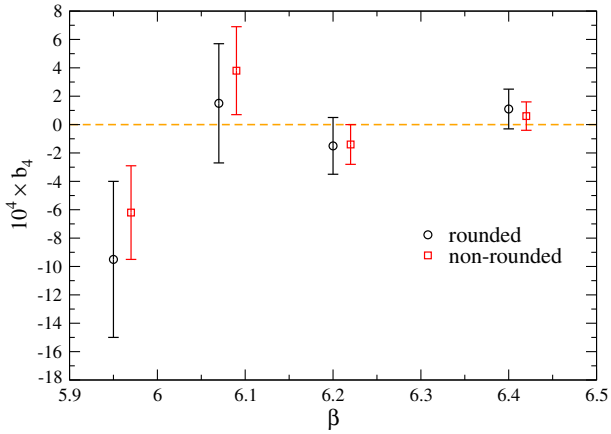

FIG. 7. Estimates of b_4 at various bare couplings.

out from the precise cancellation of higher-order terms, so that the signal-to-noise ratio is expected to scale like

$$(\chi\mathcal{V})/(\chi\mathcal{V})^{k/2} = (\chi\mathcal{V})^{(2-k)/2}.$$

This is consistent with the fact that the cumulants measure the deviations from a purely Gaussian distribution, and such deviations, because of the central limit theorem, become less and less visible as the infinite-volume limit is approached.

We conclude that the error expected in the standard determination of b_{2n} through the cumulants at $\theta = 0$ is of the order of $(\chi\mathcal{V})^n/\sqrt{N}$, where N is the size of the statistical sample, i.e. the number of independent gauge configurations. This is a particularly severe case of a lack of self-averaging [62]; for instance in the case of b_2 one has to increase the number of measurements proportionally to $\mathcal{V}^2$, in order to keep a fixed statistical accuracy as the volume is increased. Notice that this problem is not marginal. Indeed, the important parameter entering this scaling is the combination $\chi\mathcal{V}$: since $\chi^{1/4} \sim 180$ MeV $\sim (1.1$ fm$)^{-1}$, we expect a strong degradation in the signal-to-noise ratio as one approaches lattices which exceed one fermi in size, which is consistent with our observations; unfortunately, this is also at a threshold where finite-size effects are still important.

On the contrary, when using the analytic continuation approach, this problem disappears. Indeed, in this case the information about each free energy coefficient is contained also in the θ dependence of the lowest-order cumulants, including $\langle Q \rangle_{c,\theta_I}$, whose signal-to-noise ratio scales with volume as $\mathcal{V}^{1/2}$. The improvement is related to the fact that one is probing the system with an explicit nonzero external source, and is similar to that obtained when switching from the measurement of fluctuations to the measurement of the magnetization as a function of the external field in the determinations of the magnetic susceptibility of a material.

Therefore, one expects that the final statistical accuracy at a fixed number of measurements, improves when increasing the volume, rather than degrades, like for standard self-averaging quantities. Actually, in the particular case of the analytic continuation in θ, there is a slight complication related to the renormalization constant Z. This can be computed as in Eq. (18), but in this case we need also $\langle Q^2 \rangle$, whose precision scales like $\mathcal{V}^0$ with volume. The global fit method is not qualitatively better in this respect: since Z appears as a rescaling of θ it cannot be determined just by using the first cumulant; its value is fixed by the comparison of at least $\langle Q \rangle_{c,\theta_I}$ and $\langle Q^2 \rangle_{c,\theta_I}$ and the precision of the second scales as $\mathcal{V}^0$. We thus see that the best we can obtain with the analytic continuation approach is a scaling of the precision of b_{2n} with volume like $\mathcal{V}^0$; this is suboptimal with respect to the naive expectation $\mathcal{V}^{1/2}$, but still a tremendous improvement with respect to the Taylor expansion method. On the other

hand, the precisions of Z and χ scale in both approaches as $\mathcal{V}^0$.

All these scalings, and the improvement gained by analytic continuation, can be nicely seen in Fig. 3. Three determinations of Z, χ and b_2 are shown: the first one is obtained by using the Taylor expansion method, i.e. using just the $\theta = 0$ sets, the second one uses the analytic continuation approach, including in the global fit up to the fourth cumulant of the topological charge and fitting Z, χ, b_2 and b_4, while the last one follows the same strategy as the second one but b_4 is fixed to zero in the fit. The determination of b_4 obviously used only the first two methods. Actually, a reasonable comparison between different methods should proceed along the following lines: compare the errors obtained by different approaches when using the same machine time. For the comparison to be fair we thus have to rescale the statistics of the $\theta = 0$ determination by about a factor of 10, i.e. the errors of the corresponding determination by about a factor of 3. We thus see that no gain is obtained by using the analytic continuation approach to determine Z and χ, while it is extremely beneficial for b_2 and b_4, as theoretically expected.

A last point that remains to be investigated is the effectiveness, within the analytic continuation approach, of the global fit to all the cumulants with respect to the traditional procedure of using just $\langle Q \rangle_c$, with Z fixed using Eq. (18). Such a comparison is performed in Fig. 8, in which also intermediate cases are shown: a global fit of all the parameters using different numbers of cumulants or a global fit of all the parameters but Z [which was fixed by Eq. (18)], using different numbers of cumulants. As can be seen the inclusion in the fit of cumulants of order higher than the second does not improve appreciably the precision of the result; the error reduction attainable by fitting also Z instead of fixing it before the fit is not huge, but still significant. Indeed, by using all the cumulants of the topological charge and fitting Z we reduced the errors by about a factor of 2 with respect to the traditional procedure of using just $\langle Q \rangle_{\theta_I}$ with Z fixed by Eq. (18).

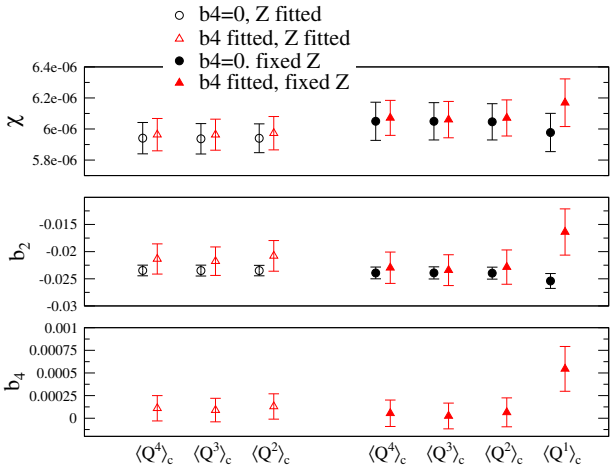

FIG. 8. Comparison between different fitting procedures in the analytic continuation approach. Data refer to the 30^4 lattice at bare coupling $\beta = 6.40$. Empty symbols are the result of a global fit procedure (in which also Z is determined) using up to the 4th, 3rd or 2nd cumulant. Full symbols are obtained using a global fit [with Z fixed by Eq. (18)] and using up to the 4th, 3rd, 2nd or 1st cumulant.

B. Some considerations about the finite-temperature case

A strategy allowing one to measure b_{2n} on arbitrary large volumes represents a substantial improvement, that permits one to gain statistical accuracy and reduces the possible systematics related to finite-size effects. There are however cases in which this possibility is not just an "improvement," but it enables the study of otherwise intractable problems. This is the case of b_2 at finite temperature for $T < T_c$. Once the lattice spacing is fixed and the temperature is fixed (i.e. β and N_t are fixed), to ensure that we are studying a finite-temperature system we have to impose the constraint $N_s \gg N_t$ (typically $N_s \gtrsim 4N_t$ is used) and this fixes a lower value for the acceptable four-volumes to be used. What typically happens is that this minimum value of $\mathcal{V}$ is large enough to make a measure of b_2 using the Taylor expansion method extremely difficult.

In order to verify that the analytic continuation approach works equally well also at finite temperature, we performed a simulation at $\beta = 6.173$ on a 10×40^4 lattice. Such a point was previously investigated in Ref. [63] using the Taylor expansion method. The result from Ref. [63], together with our new determinations and the $T = 0$ result are reported in Fig. 9. The old determination of Ref. [63] was based on a statistics of about 800 K measures: our present determination obtained via analytic continuation reaches a precision which is more than 1 order of

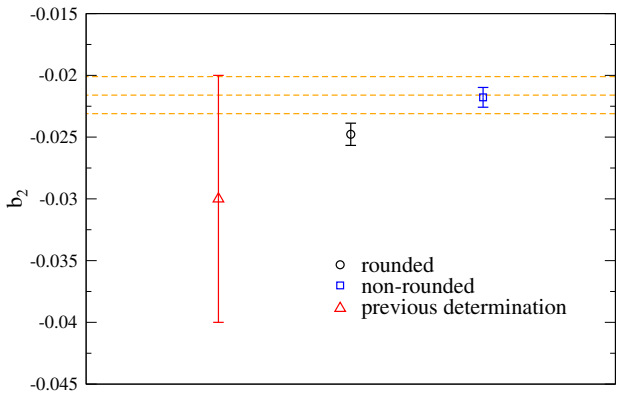

FIG. 9. b_2 value at $T \simeq 0.95 T_c$ on a 10×40^3 lattice (bare coupling $\beta = 6.173$) with a comparison of the determination in Ref. [63], obtained using the Taylor expansion method, and a new estimate obtained by using the analytic continuation method. The horizontal lines denote the $T = 0$ result.

magnitude larger, with about half the computational effort (in particular, a machine-time equivalent to around 350 K measures taken at $\theta = 0$).

Different considerations should be made for temperatures above the critical temperature T_c. Indeed, in all the recent studies of b_2 at finite temperature [63–66] (in which the Taylor expansion method was always used) it was noted that the determination of b_2 in the low-temperature phase is very difficult, while it gets abruptly easier above deconfinement. The reason for this fact is simple: we have seen that the relevant parameter for the degradation of the statistical accuracy in the determination of the cumulants at $\theta = 0$ is $\chi\mathcal{V}$. Since at the deconfinement transition the topological susceptibility steeply decreases [53,65–71], a precise determination of b_2 by the standard Taylor expansion approach becomes much easier, in the deconfined phase, even on moderately large volumes.

IV. CONCLUSIONS

In this study we have exploited numerical simulations performed at imaginary values of θ and analytic continuation in order to determine the dependence of the free energy density of the $SU(3)$ pure gauge theory on the topological parameter θ. As an improvement with respect to previous applications of the same strategy [21], we have considered a global fit to the θ dependence of various free energy derivatives, i.e. various cumulants of the topological charge distribution. That has permitted us to reach an increased precision, obtaining the following estimates for the continuum extrapolated values: $r_0\chi^{1/4} = 0.4708(42)(58)$, $b_2 = -0.0216(10)(11)$ and $|b_4| \lesssim 4 \times 10^{-4}$.

The strategy based on analytic continuation turns out to be particularly well suited for the determination of the higher-order terms, for which the traditional Taylor expansion method, based on the determination of cumulants of the topological charge distribution at $\theta = 0$, faces a severe problem when approaching large volumes, where corrections to Gaussian-like fluctuations become hardly measurable. Indeed, we have shown that the statistical error attained in the determination of b_{2n} through the cumulants at $\theta = 0$ scales with the four-dimensional volume $\mathcal{V}$, for a fixed number of measurements, like $(\chi\mathcal{V})^n$, where χ is the topological susceptibility. As we have shown, this property of analytic continuation turns out to be essential for the determination of the θ dependence right below the deconfinement temperature T_c, and hence this strategy could be adopted for a future improved determination of the change of θ dependence taking place at deconfinement [63].

ACKNOWLEDGMENTS

We thank Francesco Negro and Ettore Vicari for useful discussions. Numerical simulations have been performed on the CSN4 cluster of the Scientific Computing Center at INFN-PISA and on the Galileo machine at CINECA (under INFN project NPQCD). Work partially supported by the INFN SUMA Project.

[1] G. 't Hooft, Phys. Rev. Lett. **37**, 8 (1976).
[2] E. Witten, Nucl. Phys. **B156**, 269 (1979).
[3] G. Veneziano, Nucl. Phys. **B159**, 213 (1979).
[4] D. J. Gross, R. D. Pisarski, and L. G. Yaffe, Rev. Mod. Phys. **53**, 43 (1981).
[5] T. Schaefer and E. V. Shuryak, Rev. Mod. Phys. **70**, 323 (1998).
[6] A. R. Zhitnitsky, Nucl. Phys. **A813**, 279 (2008).
[7] M. Unsal, Phys. Rev. D **86**, 105012 (2012).
[8] E. Poppitz, T. Schaefer, and M. Unsal, J. High Energy Phys. 03 (2013) 087.
[9] M. M. Anber, Phys. Rev. D **88**, 085003 (2013).
[10] F. Bigazzi, A. L. Cotrone, and R. Sisca, J. High Energy Phys. 08 (2015) 090.
[11] E. Witten, Phys. Rev. Lett. **81**, 2862 (1998).
[12] E. Witten, Ann. Phys. (N.Y.) **128**, 363 (1980).
[13] E. Vicari and H. Panagopoulos, Phys. Rep. **470**, 93 (2009).
[14] C. R. Allton, S. Ejiri, S. J. Hands, O. Kaczmarek, F. Karsch, E. Laermann, C. Schmidt, and L. Scorzato, Phys. Rev. D **66**, 074507 (2002).
[15] R. V. Gavai and S. Gupta, Phys. Rev. D **68**, 034506 (2003).
[16] C. R. Allton, M. Doring, S. Ejiri, S. J. Hands, O. Kaczmarek, F. Karsch, E. Laermann, and K. Redlich, Phys. Rev. D **71**, 054508 (2005).
[17] V. Azcoiti, G. Di Carlo, A. Galante, and V. Laliena, Phys. Rev. Lett. **89**, 141601 (2002).
[18] B. Alles and A. Papa, Phys. Rev. D **77**, 056008 (2008).
[19] B. Alles, M. Giordano, and A. Papa, Phys. Rev. B **90**, 184421 (2014).
[20] S. Aoki, R. Horsley, T. Izubuchi, Y. Nakamura, D. Pleiter, P. E. L. Rakow, G. Schierholz, and J. Zanotti, arXiv:0808.1428.
[21] H. Panagopoulos and E. Vicari, J. High Energy Phys. 11 (2011) 119.
[22] M. D'Elia and F. Negro, Phys. Rev. Lett. **109**, 072001 (2012); Phys. Rev. D **88**, 034503 (2013).
[23] M. G. Alford, A. Kapustin, and F. Wilczek, Phys. Rev. D **59**, 054502 (1999).
[24] A. Hart, M. Laine, and O. Philipsen, Phys. Lett. B **505**, 141 (2001).
[25] P. de Forcrand and O. Philipsen, Nucl. Phys. **B642**, 290 (2002).
[26] M. D'Elia and M.-P. Lombardo, Phys. Rev. D **67**, 014505 (2003).

[27] M. D'Elia and F. Sanfilippo, Phys. Rev. D **80**, 014502 (2009).
[28] T. Takaishi, P. de Forcrand, and A. Nakamura, *Proc. Sci.*, LAT2009 (2009) 198 [arXiv:1002.0890].
[29] B. Berg, Phys. Lett. **104B**, 475 (1981).
[30] Y. Iwasaki and T. Yoshie, Phys. Lett. **131B**, 159 (1983).
[31] S. Itoh, Y. Iwasaki, and T. Yoshie, Phys. Lett. **147B**, 141 (1984).
[32] M. Teper, Phys. Lett. **162B**, 357 (1985).
[33] E.-M. Ilgenfritz, M. L. laursen, M. Müller-Preuβker, G. Schierholz, and H. Schiller, Nucl. Phys. **B268**, 693 (1986).
[34] M. Luscher, Commun. Math. Phys. **293**, 899 (2010).
[35] M. Luscher, J. High Energy Phys. 08 (2010) 071.
[36] C. Bonati and M. D'Elia, Phys. Rev. D **89**, 105005 (2014).
[37] K. Cichy, A. Dromard, E. Garcia-Ramos, K. Ottnad, C. Urbach, M. Wagner, U. Wenger, and F. Zimmermann, *Proc. Sci.*, LATTICE2014 (2014) 075 [arXiv:1411.1205].
[38] Y. Namekawa, *Proc. Sci.*, LATTICE2014 (2014) 344 [arXiv:1501.06295].
[39] C. Alexandrou, A. Athenodorou, and K. Jansen, Phys. Rev. D **92**, 125014 (2015)].
[40] P. Di Vecchia, K. Fabricius, G. C. Rossi, and G. Veneziano, Nucl. Phys. **B192**, 392 (1981).
[41] P. Di Vecchia, K. Fabricius, G. C. Rossi, and G. Veneziano, Phys. Lett. **108B**, 323 (1982).
[42] M. Teper, Phys. Lett. B **232**, 227 (1989).
[43] M. Campostrini, A. Di Giacomo, H. Panagopoulos, and E. Vicari, Nucl. Phys. **B329**, 683 (1990).
[44] A. Di Giacomo, H. Panagopoulos, and E. Vicari, Nucl. Phys. **B338**, 294 (1990).
[45] A. Di Giacomo and E. Vicari, Phys. Lett. B **275** (1992) 429.
[46] L. Del Debbio, H. Panagopoulos, and E. Vicari, J. High Energy Phys. 08 (2002) 044.
[47] M. Guagnelli, R. Sommer, and H. Wittig (ALPHA Collaboration), Nucl. Phys. **B535**, 389 (1998).
[48] R. Sommer, Nucl. Phys. **B411**, 839 (1994).
[49] M. Creutz, Phys. Rev. D **21**, 2308 (1980).
[50] A. D. Kennedy and B. J. Pendleton, Phys. Lett. **156B**, 393 (1985).
[51] M. Creutz, Phys. Rev. D **36**, 515 (1987).
[52] N. Cabibbo and E. Marinari, Phys. Lett. **119B**, 387 (1982).
[53] B. Alles, M. D'Elia, and A. Di Giacomo, Nucl. Phys. **B494**, 281 (1997); **B679**, 397(E) (2004).
[54] L. Del Debbio, L. Giusti, and C. Pica, Phys. Rev. Lett. **94**, 032003 (2005).
[55] S. Durr, Z. Fodor, C. Hoelbling, and T. Kurth, J. High Energy Phys. 04 (2007) 055.
[56] M. Luscher and F. Palombi, J. High Energy Phys. 09 (2010) 110.
[57] K. Cichy, E. Garcia-Ramos, K. Jansen, K. Ottnad, and C. Urbach (ETM Collaboration), J. High Energy Phys. 09 (2015) 020.
[58] M. Cé, C. Consonni, G. P. Engel, and L. Giusti, Phys. Rev. D **92**, 074502 (2015).
[59] J. Garden, J. Heitger, R. Sommer, and H. Wittig (ALPHA and UKQCD Collaborations), Nucl. Phys. **B571**, 237 (2000).
[60] M. D'Elia, Nucl. Phys. **B661**, 139 (2003).
[61] L. Giusti, S. Petrarca, and B. Taglienti, Phys. Rev. D **76**, 094510 (2007).
[62] A. Milchev, K. Binder, and D. W. Heermann, Z. Phys. B **63**, 521 (1986).
[63] C. Bonati, M. D'Elia, H. Panagopoulos, and E. Vicari, Phys. Rev. Lett. **110**, 252003 (2013).
[64] C. Bonati, J. High Energy Phys. 03 (2015) 006.
[65] S. Borsanyi, M. Dierigl, Z. Fodor, S. D. Katz, S. W. Mages, D. Nogradi, J. Redondo, A. Ringwald, and K. K. Szabo, Phys. Lett. B **752**, 175 (2016).
[66] G. Y. Xiong, J. B. Zhang, Y. Chen, C. Liu, Y. B. Liu, and J. P. Ma, Phys. Lett. B **752**, 34 (2016).
[67] C. Gattringer, R. Hoffmann, and S. Schaefer, Phys. Lett. B **535**, 358 (2002).
[68] B. Lucini, M. Teper, and U. Wenger, Nucl. Phys. **B715**, 461 (2005).
[69] L. Del Debbio, H. Panagopoulos, and E. Vicari, J. High Energy Phys. 09 (2004) 028.
[70] E. Berkowitz, M. I. Buchoff, and E. Rinaldi, Phys. Rev. D **92**, 034507 (2015).
[71] R. Kitano and N. Yamada, J. High Energy Phys. 10 (2015) 136.